Dynamic particle aggregation in the bimolecular $A+B\rightarrow 0$ reaction

V. Kuzovkov
Department of Theoretical Physics, University of Latvia, Riga, Latvia

E. Kotomin
Institute for Solid State Physics, University of Latvia, 19 Rainis Blvd., Riga, Latvia

(Received 22 October 1992; accepted 17 February 1993)

The effect of an elastic ($U=-\lambda/r^3$) interaction between *similar* particles on the kinetics of the bimolecular $A+B\rightarrow 0$ reaction is studied for the first time in terms of a novel formalism of the many-point particle densities taking into account the spatial correlations of *both* similar and dissimilar particles. It is shown that an elastic attraction results in the *dynamic* aggregation of similar particles and therefore in the reduced reaction rate unusual for the standard chemical kinetics. The distinctive time of such aggregate formation depends on the initial particle concentration and on their spatial distribution but is always considerably shorter than that for *statistical* aggregation of similar noninteracting particles. The latter is a distinctive feature of the self-organization in bimolecular reactions at long times and/or great particle concentrations. For the same value of the interaction parameter λ an attraction of similar particles has a greater impact on the reaction kinetics than that of dissimilar particles.

I. INTRODUCTION

As is well known, point defects in solids interact with each other even if they are not charged with respect to the crystalline lattice. This *elastic* interaction arises due to overlap of displacement fields of the two close defects and falls off with a distance r between them as $U(r)=-\lambda r^{-6}$ for two symmetric (isotropic) defects in an isotropic crystal or as $U(r)=-\lambda\alpha_4 r^{-3}$, if the crystal is weakly anisotropic[1,2] (α_4 is the angular dependent cubic harmonic with $l=4$). In the latter case, due to presence of the cubic harmonic α_4 an interaction is attractive in some directions but turns out to be repulsive in other directions. Finally, if one or both defects are anisotropic, the angular dependence of $U(\mathbf{r})$ cannot be presented in an analytic form.[3] The role of the elastic interaction within pairs of the complementary radiation Frenkel defects in metals (vacancy-interstitial atom) was studied in Refs. 4–6, it was shown to have considerable impact on the kinetics of their recombination, $A+B\rightarrow 0$.

The elastic interaction between defects was studied also in alkali halide crystals; in particular, for primary Frenkel defects, the so-called F and H centers (anion vacancy trapped an electron and interstitial halogen atom forming a quasimolecule X_2^- with a regular anion X^- nearby). Since the latter are anisotropic, the interaction decays as r^{-3}; the elastic constant was calculated to be $\lambda\approx 3$ eV Å^{-3} in KBr.[7] Taking into account that H centers become mobile above 30 K (Ref. 8), we obtain that the distinctive dimensionless parameter $r_e=\sqrt[3]{\lambda/k_BT}=\sqrt[3]{\beta\lambda}\gg r_0$ (the annihilation radius, which is close to the interionic spacing) and therefore the elastic interaction is expected to play an essential role in alkali halides too. (F centers in alkali halides are immobile below room temperature.) The role of elastic defect interaction in alkali halides was studied in Refs. 9–14. Since an H center starts to rotate on a lattice site already at 10 K (Ref. 8), i.e., much before it starts to migrate, one can reasonably assume that when approaching F center, it takes energetically the most favorable orientation corresponding to the attraction and thus one may consider hereafter F, H interaction as *isotropic* attraction. Note also that careful variational calculations[4] have also demonstrated that mobile interstitials in metals avoid the repulsive directions around vacancies and recombine approaching them from another side, which effectively results in an isotropic attraction with the recombination radius corrected by a factor close to 0.5.

Mobile H centers in alkali halides are known to aggregate in a form of complex hole centers;[15] this process is stimulated by elastic attraction. It was estimated[16,17] that for such *similar* defect attraction the elastic constant λ is larger by a factor of 5 than that for dissimilar defects: F, H centers. Therefore, elastic interaction has to play a considerable role in the colloid formation in alkali halides observed at high temperatures.[18]

To our knowledge, until now an interaction between *similar* defects (particles) AA or BB during their bimolecular $A+B\rightarrow 0$ reactions (Frenkel defect recombination) was neglected, unlike interaction between dissimilar defects AB. (The only exception is the paper[19] dealing with Coulomb interaction of similar particles.) The traditional approach for describing this kinetics[20,21] is based on a simple mathematical scheme. The basic equation for macroscopic concentrations $n_A=n_B=n(t)$ (the so-called *law of mass action*) is completed with the time-dependent reaction rate $K=K(t)$ which is a functional linear in the joint correlation function of dissimilar paticles $Y(r,t)$:

$$\frac{dn(t)}{dt}=-K(t)n^2(t), \tag{1}$$

$$K(t)=4\pi\int_0^\infty \sigma(r)\,Y(r,t)r^2\,dr. \tag{2}$$

In its turn, this correlation function is a solution of the linear kinetic equation

$$\frac{\partial Y(r,t)}{\partial t}=D\nabla(\nabla Y(r,t)+\beta Y(r,t)\nabla U_{AB}(r))$$
$$-\sigma(r)\,Y(r,t) \tag{3}$$

with the boundary condition improsed $Y(\infty,t)=1$ (the correlation weakening for well-separated particles). The quantities $\sigma(r)$ and $U_{AB}(r)$ entering Eqs. (2) and (3) are the recombination rate and interaction potential of dissimilar particles AB separated by a distance r; $\beta=1/k_BT$, and $D=D_A+D_B$ is the coefficient of relative diffusion. Let us describe the defect recombination in terms of generally accepted *black-sphere model*;[22] i.e., AB pairs disappear instantly approaching to within a critical distance r_0 (annihilation radius). In this model the second term in on the right-hand side of Eq. (3) is omitted, this equation is solved in the interval $r>r_0$ and the reaction rate is defined by the flux of particles through the recombination sphere, which is defined by the gradient of the correlation function at the edge of the recombination sphere, i.e., $K(t)=4\pi Dr_0^2\,\partial Y(r,t)/\partial r$ at $r=r_0$. The typical problem statement is to find the *steady-state* reaction rate, $K_0=K(\infty)$; it could be solved using the linear time-independent partial differential Eq. (3).

It is self-evident that Eqs. (1)–(3) neglect any interaction of *similar* particles; the partial diffusion coefficients enter here only as a sum D, and potentials $U_{AA}(r)$, $U_{BB}(r)$ are also absent. As was noted for the first time in Ref. 23, an incorporation of the relative distribution of similar particles in the kinetics of bimolecular reactions gives rise to a *nonlinear many-particle effect* which requires a new more complete level of the correlation treatment including, along with the joint functions $Y(r,t)$ mentioned above, the analogous joint functions $X_A(r,t)$, $X_B(r,t)$ for *similar* particles.

Such an approach which has been developed in[24,25] results in qualitatively new concepts unusual for standard chemical kinetics. For example, a search of the *stationary* reaction rate K_0 as a functional of $\sigma(r)$ and $U_{AB}(r)$ becomes now meaningless since $K(t)$ tends to zero, as $t\rightarrow\infty$. For neutral particles A,B the *statistical aggregation of similar particles* takes place: recombination of dissimilar particles leads to the pattern formation,[24–37] i.e., a whole reaction volume is divided in time into alternating A- or B-rich domains with the linear size $\xi=\sqrt{Dt}$. [If recombination was absent, $\sigma(r)\equiv 0$, the only reason for such a structure with loose aggregates could arise from an attraction between similar particles.] Similar particle aggregation in the $A+B\rightarrow 0$ reaction was found to be an *universal effect* which was studied in detail both analytically and by means of computer simulations; it takes place under both particle creation due to their permanent-source (irradiation) and further concentration decay.[24,25,28–30,35,38,39] Such a statistical particle aggregation affects considerably the asymptotic kinetics of the concentration decay; instead of the standard result $n(t)\propto t^{-1}$ [Eqs. (1) to (3)] the reduced rate, $n(t)\propto t^{-3/4}$, of the diffusion-controlled 3D decay is observed. In fact, it is quite similar to the self-organization phenomena studied in synergetics,[40] but here on the *microscopic* (atomic) length scale.

In this paper, we consider the following problem. Defects B are mobile ($D_B>0$) and interact with each other elastically as $U_{BB}(r)=-\lambda r^{-m}$ ($m=3$ for the elastic interaction); we call hereafter this interaction as *dynamical* one. Their counter-partners A involved into the bimolecular recombination, $A+B\rightarrow 0$, could be both immobile, $D_A=0$, and mobile, $D_A=D_B$. To calculate the kinetics of this reaction, obviously we have to go beyond the framework of the traditional approach, Eqs. (1)–(3), which neglects the interaction of similar particles.

The plan of the paper is as follows. In Sec. II the adequate mathematical formalism based on the joint densities of *both* similar AA, BB, and dissimilar AB particles is presented. The interaction potentials are discussed in Sec. III. The results obtained are presented in Sec. IV. It is demonstrated that the dynamical interaction between similar defects leads to their *dynamic* aggregation, qualitatively similar to the above-discussed *statistical* aggregation of noninteracting particles. However, it is shown that these two effects are well separated in time. Lastly, main conclusions of this investigation emphasizing the importance of taking into account the elastic defect interaction in solids are presented in Sec. V.

II. BASIC KINETIC EQUATIONS

Let us restrict ourselves to the treatment of kinetics in terms of the above-discussed *black-sphere model*;[22] i.e., AB pairs disappear instantly. We assume equal defect concentrations, $n(t)=n_A=n_B$. It is convenient to use the dimensionless units: $r'=r/r_0$, $t'=Dt/r_0^2$, $K'(t')=K(t)/4\pi Dr_0$, $n'(t')=4\pi r_0^3 n(t)$ and relative diffusion coefficients $\mathscr{D}_A=2\kappa$, $\mathscr{D}_B=2(1-\kappa)$ where $\kappa=D_A/D$. Primes are omitted below. The time development of the dimensionless defect concentration coincides formally with Eq. (1) whereas the dimensionless reaction rate is essentially simplified being defined now just the gradient through recombination sphere with the unity radius:

$$K(t)=\left.\frac{\partial Y(r,t)}{\partial r}\right|_{r=1}. \tag{4}$$

The joint correlation functions describing spatial correlations of dissimilar, $Y(r,t)$, and similar, $X(r,t)$, defects obey the following nonlinear kinetic equations[19,23,24]

$$\frac{\partial Y(r,t)}{\partial t}=\nabla(\nabla Y(r,t)+Y(r,t)\nabla\mathscr{U}_{AB}(r,t))$$
$$-n(t)K(t)Y(r,t)\sum_{\nu=A,B}J[X_\nu], \tag{5}$$

$$\frac{\partial X_A(r,t)}{\partial t}=\mathscr{D}_A\nabla(\nabla X_A(r,t)+X_A(r,t)\nabla\mathscr{U}_{AA}(r,t))$$
$$-2n(t)K(t)X_A(r,t)J[Y], \tag{6}$$

$$\frac{\partial X_B(r,t)}{\partial t}=\mathscr{D}_B\nabla(\nabla X_B(r,t)+X_B(r,t)\nabla\mathscr{U}_{BB}(r,t))$$
$$-2n(t)K(t)X_B(r,t)J[Y]. \tag{7}$$

In Eqs. (5)–(7) dimensionless potentials $\mathscr{U}_{AA}$, $\mathscr{U}_{BB}$, and $\mathscr{U}_{AB}$ are defined by β times the potential of mean force, which bulky expressions were given in Ref. 19. By definition,[24] the joint correlation functions give a ratio of the probability density to find pair of defects $\nu\nu'$ ($\nu,\nu'=A,B$) at a given relative distance r to that for a random distribution, $r\rightarrow\infty$, that is these functions are normalized *asymptotically* as $X_\nu(r\rightarrow\infty,t)=1$, $Y(r\rightarrow\infty,t)=1$ (the Poisson distribution) and an instant annihilation leads to the condition $Y(r\leqslant r_0,t)\equiv 0$. The boundary conditions for similar particles are discussed in detail in Refs. 19 and 24.

The nonlinear terms of these equations arise after use of the superposition Kirkwood approximation;[41] the functionals J [in Eqs. (5) to (7)] are defined as

$$J[Z]=\frac{1}{2r}\int_{|r-1|}^{r+1}(Z(r',t)-1)r'dr', \quad Z=X,Y. \tag{8}$$

In the formal limit of the infinitely diluted system ($n(t)\rightarrow 0$) the dimensionless interaction potential $\mathscr{U}(r,t)=\beta U(r)$; it is another source of the nonlinearity in the kinetic equations. In this limiting case Eq. (5) transforms into well-known in the standard kinetics Eq. (3) modified for the black-sphere model of recombination, as was described above. This demonstrates the relation between traditional and our many-particle approaches. In turn, the equations for the similar correlation functions X_ν ($\nu=A,B$) are decoupled off the complete set of kinetic equations and thus do not affect no longer the reaction kinetics. Their steady-state solution ($t\rightarrow\infty$) is the Boltzmann distribution

$$X_\nu^0(r)=X_\nu(r,\infty)=\exp[-\beta U_{\nu\nu}(r)]. \tag{9}$$

In this paper, we take into account the nonlinear terms in the kinetic equations containing functionals J (coupling spatial correlations of similar and dissimilar particles) but neglect the perturbation of the pair potentials assuming that $\mathscr{U}(r,t)=\beta U(r)$. This is justified in the diluted systems and for the moderate particle interaction which holds for low defect densities and loose aggregates of similar defects. However, potentials of mean force have to be taken into account for strongly interacting particles (defects) and under particle accumulation when colloid formation often takes place.[18]

III. INTERACTION POTENTIALS

Following arguments of Sec. I, we consider the *isotropic* attraction, $U(r)=-\lambda r^{-3}$. In terms of mechanics this long-range potential is characterized by an infinite action radius, but in the kinetics it results in the *effective recombination radius*. In the traditional approach[4,5] it is $R_{\text{eff}}=3r_e/\Gamma(1/3)=1.12\sqrt[3]{\lambda\beta}$ (Γ is gamma function), i.e., decays with the temperature as $T^{-1/3}$. (To distinguish the elastic interactions within different pairs of defects, say *AA, BB* and *AB, several* radii r_e could be used.) The Boltzmann distribution, Eq. (9), could be rewritten as $X^0(r)=\exp[(r_e/r)^3]$; it shows how the dynamic interaction leads to the increased concentration of close similar particles, at $r\leqslant r_e$, as compared to their Poisson (random) distribution, $X\equiv 1$. Keeping in mind that the law $U(r)=-\lambda r^{-3}$ holds only asymptotically and fails for nearest neighbors, $r\leqslant a_0$ (a_0 is the interionic spacing), let us introduce the cutoff potential: $U(r)=-\lambda r_0^{-3}$ as $r\leqslant r_0$. It means that we use in Eqs. (5)–(7) the dimensionless potentials

$$\mathscr{U}=\begin{cases}-(r_e/r_0)^3, & r<r_0,\\ -(r_e/r_0)^3\dfrac{1}{r^3}, & r\geqslant r_0.\end{cases} \tag{10}$$

The ratio r_e/r_0 entering the Eq. (10) is the distinctive parameter, defining the effect of dynamic particle aggregation. Remember that the statistical aggregation, arising due to many-particle effects, is characterized by another spatial scale—the so-called *diffusion length* $\xi=\sqrt{Dt}$ (Refs. 23 and 24). Therefore, the recombination kinetics under study is governed by an *interplay* of these two parameters and depending on the reaction time t, both cases $\xi<r_e$ and $\xi>r_e$ are possible. In *both* kinds of aggregation the joint correlation function $X(r,t)$ at small relative distances r exceeds considerably the asymptotic value of the unity and thus it is not a trivial task to distinguish these two competing effects.

IV. RESULTS

A. Immobile *A* particles

In calculations presented in this section we assume one kind of defects to be immobile ($D_A=0$, $\kappa=0$) and their dimensionless initial concentration $n(0)=0.1$ is not too high; it is less than 10% of the defect saturation level accumulated after prolonged irradiation.[25] Its increase (decrease) does not affect the results qualitatively but shorten (lengthen, respectively) the distinctive times when the effects under study are observed. To stress the effects of defect mobility, we present in parallel in Secs. IV A and IV B results obtained for immobile particles A ($D_A=0$, *asymmetric case*) and equal mobility of particles A and B ($D_A=D_B$, *symmetric case*). In both cases only pairs of similar particles BB interact via elastic forces, Eq. (10), but not AA or AB. The initial distribution ($t=0$) of all defects is assumed to be random

$$Y(r>1,0)=X_\nu(r,0)=1, \quad \nu=A,B. \tag{11}$$

In Fig. 1(a) the decay of the defect concentration vs time is shown. (Note that all parameters given hereafter are dimensionless.) In the standard chemical kinetics, Eqs. (1)–(3), the reaction rate is time-dependent only at short times (Ref. 22)

$$K(t)=4\pi Dr_0\left(1+\frac{r_0}{\sqrt{\pi Dt}}\right). \tag{12}$$

The dotted curve gives results for the integrated Eq. (1) in conjunction with Eq. (12), whereas the full curves 1 to 3 are calculated for different values of the parameter r_e/r_0. Curve 1 coincides practically with that for $r_e=0$, i.e., for the case of noninteracting particles. In other words, deviation of the full curve at long times from that for the standard kinetics demonstrates the above-discussed reduc-

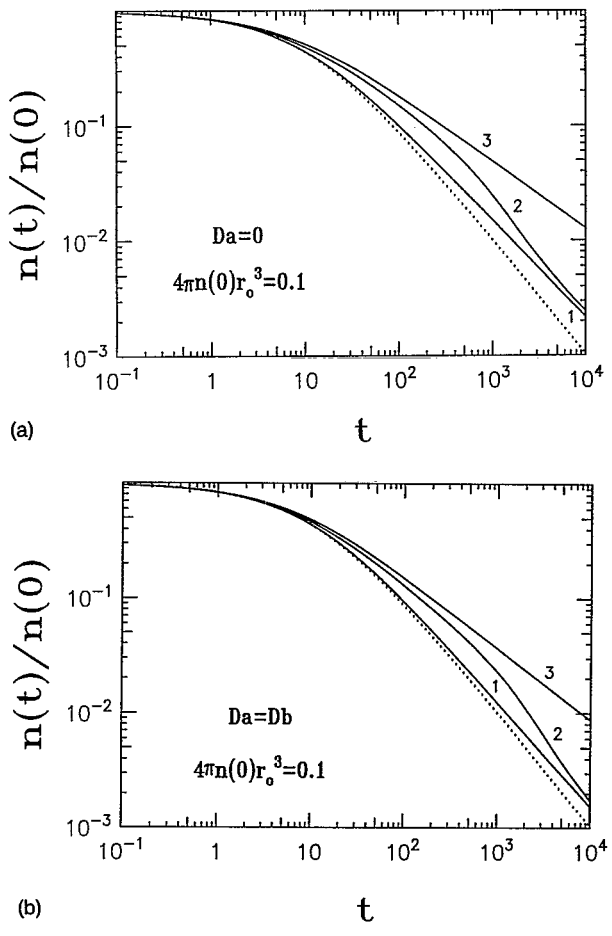

FIG. 1. The decay in time of the macroscopic particle concentration for asymmetric (a) and symmetric (b) cases corresponding to $D_A=0$ and $D_A=D_B$, respectively. The initial concentration $n(0)=0.1$. Parameter r_e/r_0: 1(1); 2(2); 3(3). Full curves show many-particle effects, whereas dotted line shows results of their neglect.

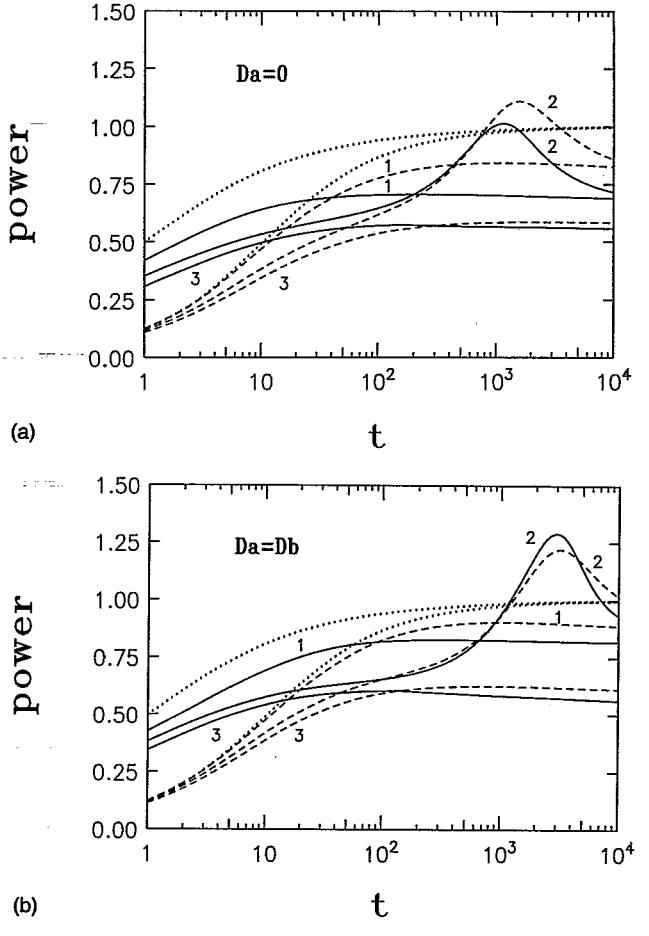

FIG. 2. The critical exponent of the power decay law, Eq. (12), as a function of time for asymmetric (a) and symmetric (b) cases. The initial particle concentrations $n(0)$: 1.0 (solid curves), 0.1 (dashed curves). Dotted lines are obtained neglecting the many-particle effects. Parameter r_e/r_0: 1(1); 2(2); 3(3).

tion of the reaction rate caused by the *statistical* aggregation of similar particles. In turn, curve 2 for $r_e/r_0=2$ considerably deviates from curve 1 at the *intermediate* times $10^1<t<10^3$ due to the contribution of the *dynamic* aggregation. At longer times these two curves tend to coincide again thus demonstrating unimportance of the dynamic effects. Finally, curve 3 calculated for a strong mutual attraction of B particles, $r_e/r_0=3$, shows a considerable reduction of the reaction rate (in a given time interval); it will approach the curve 1 only at very long times.

These results could be complemented well with the curve slopes in the double logarithmic coordinates as plotted in Fig. 2(a). Let us introduce the intermediate *critical exponent* characterizing the power-law of concentration decay

$$\alpha(t)=-\frac{d\ln n(t)}{d\ln t}. \tag{13}$$

In the traditional scheme, Eqs. (1)–(3), its asymptotic limit $\alpha_0=\alpha(\infty)=1$ is achieved already during the presented dimensionless time interval, $t\approx 10^4$. For noninteracting particles and if one of two kinds is immobile, $D_A=0$, it was earlier calculated analytically[24] that the critical exponent is additionally reduced down to $\alpha_0=0.5$. However, for a weak interaction (curve 1) it is observed that in the time interval $t\leqslant 10^4$ $\alpha_{\max}\approx 0.8$ is achieved only for a given $n(0)=0.1$, i.e., the reaction rate is *reduced* as compared to the standard chemical kinetics without particle interaction (the dotted curve). In contrast, curve 3 (strong interaction) shows a rapid transition to the analytically expected value of $\alpha_0=0.5$. In turn, the intermediate value of $r_e/r_0=2$ (curve 2) demonstrates nontrivial *nonmonotonous* transition at about $t\approx 10^3$ between the two intermediate asymptotic values of power law with $\alpha=0.50$ and $\alpha_0=0.75$. Increase in initial concentration leads to a faster transition to the critical exponent limit, $t\rightarrow\infty$.

The origin of this unusual behavior is partly clarified from Fig. 3(a) where the relevant curves 2 demonstrate the same kind of the nonmonotonous behavior as the critical exponents above. Since, according to its definition, Eq. (4), the reaction rate is a functional of the joint correlation function, this nonmonotonicity of curve 2 arises due to the spatial rearrangements in defect structure. It is confirmed by the correlation functions shown in Fig. 4(a). The dis-

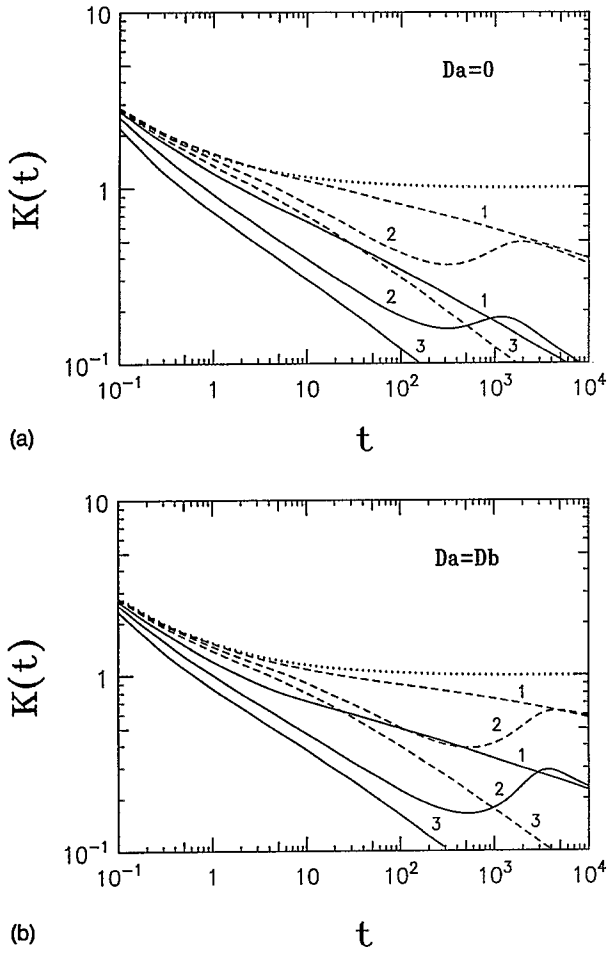

FIG. 3. The dimensionless reaction rate as a function of time for asymmetric (a) and symmetric (b) cases. Notations and parameters as in Fig. 1.

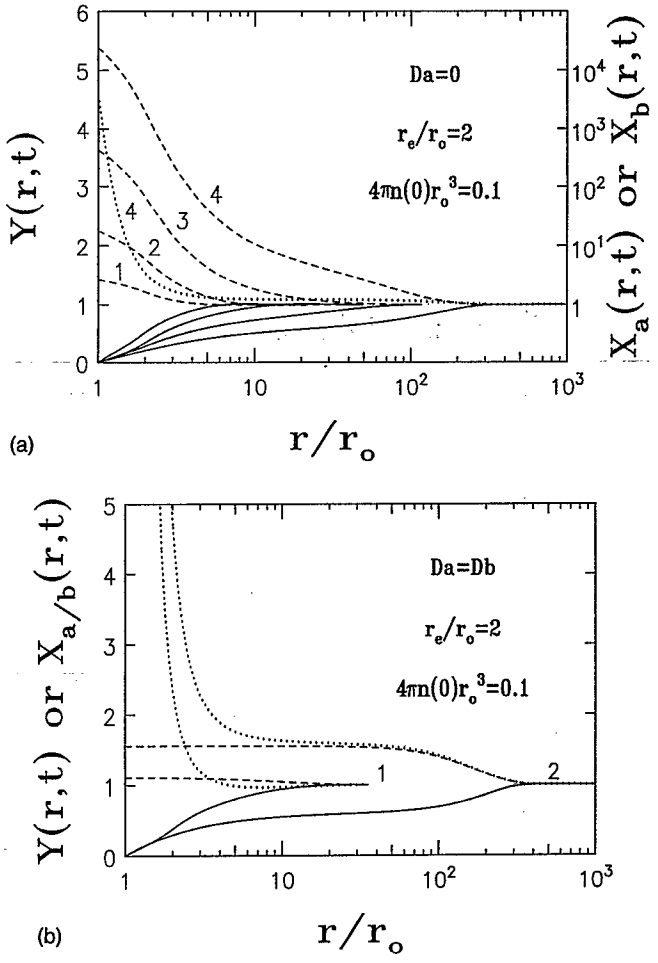

FIG. 4. The joint correlation functions for dissimilar particles $Y(r,t)$ (solid curves), immobile similar particles $X_A(r,t)$ (dashed curve) and mobile particles $X_B(r,t)$ (dotted curve). Parameters used are given. The dimensionless time (in units r_0^2/D) is (a) $t=10^1$ (1); 10^2 (2); 10^3 (3); 10^4 (4); (b) $D_A=D_B$, $t=10^2$ (1); 10^4 (curve 2).

tribution of BB pairs is quasistationary, $X_B(r,t)\approx X^0(r)=\exp[(r_e/r)^3]$, which describes their dynamic aggregation. (The only curve is plotted for X_B in Fig. 4(a) for $t=10^2$ (the dotted line) since for other time values X_B changes no more than by 10%.) This quasisteady spatial particle distribution is formed quite rapidly; already at $t\approx 10^0$ it reaches the maximum value of $X_B(r,t)\approx 10^3$. The effect of the statistical aggregation practically is not observed here, probably, due to the diffusion separation of mobile B particles.

The behavior of the correlation functions of immobile defects X_A is less obvious. The monotonous increase of its maximum with time shown in Fig. 4(a) means a strong A aggregation, but now it has the *statistical* nature. Maximum of the critical exponent in curve 2 of Fig. 2(a) corresponds to the time interval $t\approx 10^3$–10^4 when the values of both X_A and X_B become of the same order of magnitude. At longer times the reaction kinetics is defined by the relative distribution of A particles only; if the dynamic aggregation of particles B is characterized by a *single* parameter r_e, the time development of $X_A(r,t)$ shows a formation of the spatial scale (where X_A deviates from its asymptotic value of unity) which could be associated with the diffusion length $\xi=\sqrt{Dt}$. The same scale is also clearly seen for the joint density of *dissimilar* defects $Y(r,t)$. However, from these results we cannot make a final conclusion which of the two factors [i.e., an increase of the $X_A(r,t)$ maximum or the formation of the diffusion length ξ] is responsible for the transition from the kinetic stage (dynamic particle aggregation) to the stage of the statistical A aggregation. So strong increase in the maximum of $X_A(r,t)$ is defined entirely by a great asymmetry in the diffusion coefficients of particles D_A and D_B. Therefore, to answer this question, a more general case when both kinds of defects are mobile should be analyzed, which is done in the next subsection.

B. Equally mobile *A* and *B* particles

From general consideration one can expect that A-rich aggregates will be essentially destroyed by the motion of A particles which should be also accompanied with the reduced $X_A(r,t)$ maximum at short distances; this effect is indeed observed in Fig. 4(b).

To check these ideas numerically, the calculations presented in subsection A were repeated for the case $D_A=D_B$ and the results obtained are plotted in Figs. 1(b) to 4(b),

respectively. (It should be remembered that particles A do not interact dynamically.) The conclusion suggests itself that the symmetric case does not quantitatively differ from the asymmetric one, when one kind of defects was immobile. The main difference is that for weak dynamic interactions, $r_e/r_0=1$ (curves 1), the asymptotic magnitude of the critical exponent shown in Fig. 2(b) tends to change from the value of $\alpha=0.5$ to $\alpha=0.75$ analytically calculated in Ref. 24. This effect is well seen also in Fig. 1(b) where particle concentrations decay faster than in the asymmetric case, Fig. 1(a). The reaction rates shown in Fig. 3(b) exceed always the same value in Fig. 3(a) and for the intermediate values $r_e/r_0=2$ reveal quite similar nonmonotonic character. However, for a given time interval and the initial concentration $n(0)=0.1$ the critical exponent does not reach this limiting value and one observes just some acceleration of the reaction as compared to the previous case of $D_A=0$.

Of greater interest is the behavior of the joint correlation functions presented in Fig. 4(b). At any reaction time $X_B(r,t)>X_A(r,t)$ holds; now an increase of the maximum of $X_A(r,t)$ in time is very slow. According to the estimates[24] for neutral noninteracting particles, it has the logarithmic character:

$$X_A(r,t)=1+\text{const}(\ln t)^2\exp\left(-\frac{r^2}{4D_A t}\right). \tag{14}$$

The deviation of the joint correlation function X_B from X_A arises due to the additional effect of the *dynamic* aggregation, which is observed mainly at the relative distances $r\leqslant r_e$. It follows from Eq. (14), that the joint density of similar interacting particles A exceeds its asymptotic value for distances less than the correlation length $r\leqslant\xi=\sqrt{Dt}$. It is clearly seen from Fig. 4(b) that ξ is the *common* length scale for *all* correlation functions, both X and Y.

The whole reaction volume at long times may be qualitatively considered as consisting of domains with the linear size ξ, each domain has particles of one kind only, A or B Refs. 24 and 28. Particles A are distributed inside such domains randomly [which follows from the fact that $X_A(r,t)\approx$const, as $r<\xi$]. In contrast, the spatial distribution of particles B reveals an additional structure formation at $r<r_e$ caused by the dynamic interaction: large B domains contain inside themselves small dynamic aggregates with the distinctive sizes r_e. Since the reaction rate is defined by the recombination of the two kinds of particles on the common boundaries of the nearest domains (which reduces the reaction rate), such an *internal* structure of domains cannot affect the kinetics under study.

Therefore, in the symmetric situation, $D_A=D_B$, the recombination kinetics may be also separated into two stages of dynamic and statistical aggregation. At long times the particle density in these aggregates (domains), characterized by the maximum values of the correlation functions $X_\nu(r\rightarrow 0,t)$, is not very high. The reaction rate is governed by the ratio of two distinctive spatial scales $-\xi$ and r_e.

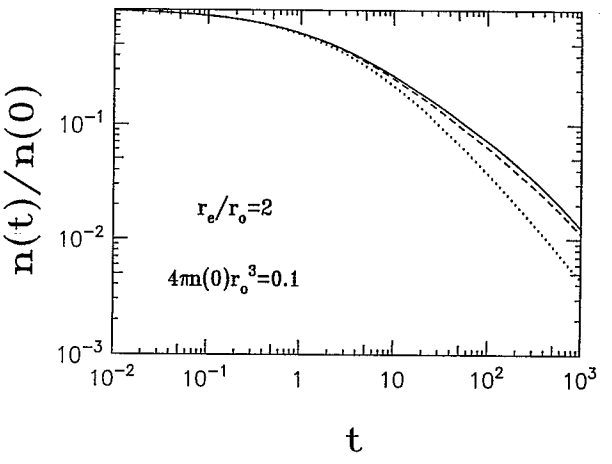

FIG. 5. The defect concentration vs time. The dotted line shows neglect of the similar particle correlation; in the solid line it is incorporated for the case $D_A=0$ and in the dashed line, for the $D_A=D_B$ case. The elastic interaction constant λ of similar and dissimilar particles is the same; $U_{AB}=U_{BB}=-\lambda r^{-3}$, whereas $U_{AA}=0$.

C. An elastic attraction of dissimilar particles

As it was mentioned above, up to now only the dynamic interaction of dissimilar particles was treated regularly in terms of the standard approach of the chemical kinetics, Eqs. (1) and (4)–(7) of our generalized approach discussed above allow us for the first time to *compare effects* of dynamic interactions between similar and dissimilar particles. Let us assume that particles A and B attract each other according to the law $U_{AB}(r)=-\lambda r^{-3}$, which is characterized by the elastic reaction radius $r_e=(\beta\lambda)^{1/3}$. The attraction potential for BB pairs is the same at $r>r_0$ but as earlier it is cutoff, as $r\leqslant r_0$. Finally, pairs AA do not interact dynamically. Consider now again the symmetric and asymmetric cases.

In the standard approach, Eqs. (1)–(3), the relative diffusion coefficient D_A/D and the potential $U_{BB}(r)$ do not affect the reaction kinetics; besides at long times the reaction rate tends to the steady-state value of $K(\infty)\propto r_e$.

The results of the incorporation of AB attraction into the kinetic equations are plotted in Figs. 5–7. The decay of the defect concentration shown in Fig. 5 demonstrates competition of the effects of the elastic interaction of similar and dissimilar particles. A comparison of the dotted lines in Fig. 5 and Figs. 1(a) and 1(b) shows clearly reaction acceleration due to mutual attraction of dissimilar particles. The correlation of the spatial distribution of similar particles is neglected in these dotted lines. The incorporation of the attraction of similar particles (full and broken curves in Fig. 5) demonstrates quite opposite effect of the reaction reduction caused by their aggregation. It leads to the *lowered* reaction rate (Fig. 6); this effect is greater for the asymmetric case. Since the dynamic and statistical particle aggregations change the reaction rate, use here of the traditional Eqs. (1)–(3) for interpretation of the experimental kinetics (e.g., for obtaining the r_e value) may lead to the considerable systematic errors.

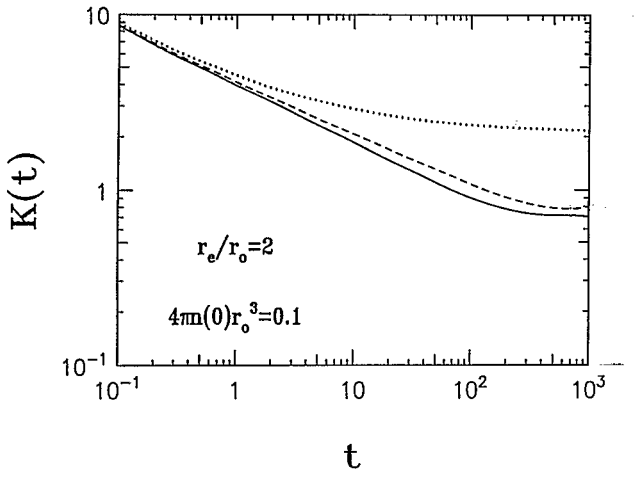

FIG. 6. The dimensionless reaction rate vs time. Notations as in Fig. 5.

As earlier for the case $U_{AB}=0$ (Fig. 4), the correlation functions $X_A(r,t)$ and $Y(r,t)$ shown in Figs. 7(a) and 7(b) demonstrate appearance of the *domain structure* in a reaction volume with interacting particles, having the distinctive size $\xi = \sqrt{Dt}$. Interaction within AB pairs holds at the relative distances $r \leqslant r_e$ (at long times $r_e < \xi$ takes place) and only slightly modifies the AB pair distribution on the domain boundaries, where the reaction takes place, but do not influence essentially the entire mechanism of the domain formation (the effect of *statistical aggregation*).

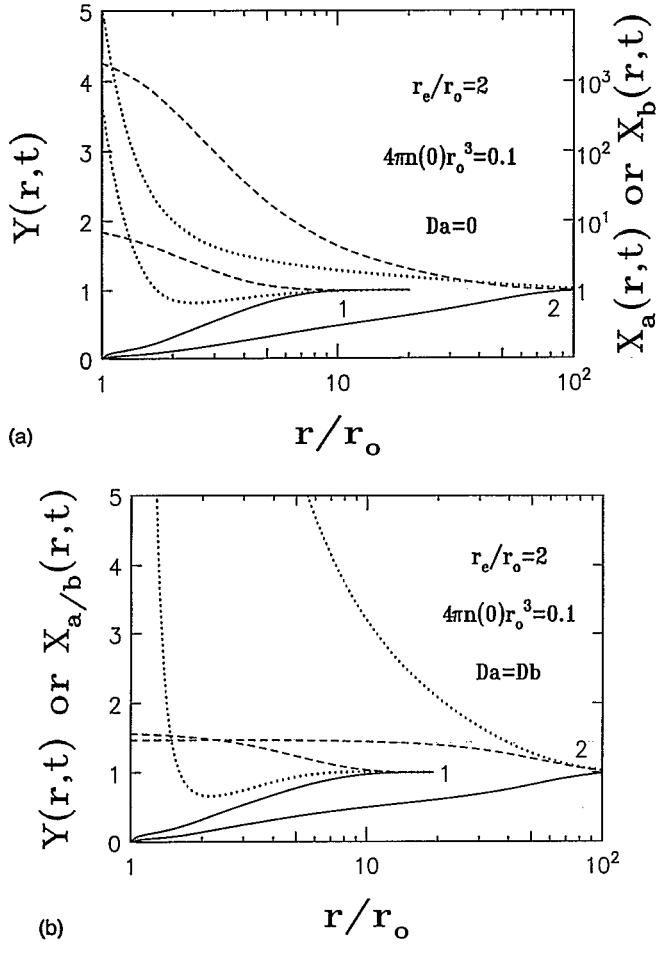

FIG. 7. The joint correlation function for the asymmetric (a) and symmetric (b) cases. Full curves are $Y(r,t)$; broken curves $X_A(r,t)$; dotted curves $X_B(r,t)$. Dimensionless time is 10^1 (1); 10^3 (2). Note that $U_{AA}=0$.

V. CONCLUSION

The elastic attraction of *similar* defects (reactants) leads to their *dynamic* aggregation which, in turn, reduces considerably the reaction rate. This effect is the most pronounced for the *intermediate* times (dependent on the initial defect concentration and spatial distribution), when the effective radius of the interaction $r_e = \sqrt[3]{\beta\lambda}$ exceeds greatly the diffusion length $\xi = \sqrt{Dt}$. In this case the reaction kinetics is governed by the elastic interaction of *both* similar and dissimilar particles. A comparative study shows that for equal elastic constants λ the elastic attraction of *similar* particles has greater effect on the kinetics than interaction of dissimilar particles.

At longer times, when $r_e \ll \xi$, the effect of the *statistical* aggregation of similar particles begins to dominate, which takes also place for both neutral noninteracting particles.[24] At this stage the reaction leads to the formation of $A(B)$-rich domains with the linear size ξ; in turn, these domains are structured *inside* themselves into smaller blocks having the typical size of r_e, which however, no longer affects the kinetics.

ACKNOWLEDGMENTS

One of us (V. K.) is greatly indebted to the Alexander von Humboldt Foundation for financial support. E.K. thanks Professor A. Blumen, Professor A. Seeger, and I. Sokolov for stimulating discussions.

[1] J. D. Eshelby, Solid State Phys. **3**, 79 (1956).
[2] H. E. Schaefer and H. Kronmüller, Phys. Status Solidi **67B**, 63 (1975).
[3] W. Scheu, W. Frank, and H. Kronmüller, Phys. Status Solidi **82B**, 523 (1977).
[4] K. Schröder and K. Dettman, Z. Phys. B **22**, 343 (1975).
[5] K. Schröder, Jülich Report No. 1083-FF, 1974.
[6] M. H. Yoo and W. H. Butler, Phys. Status Solidi **77B**, 181 (1977).
[7] K. Bachmann and H. Peisl, J. Phys. Chem. Solids **31**, 1525 (1970).
[8] M. N. Kabler, in *Point Defects in Solids*, edited by J. Crawford (New York, Plenum, 1972), p. 327.
[9] E. A. Kotomin and I. I. Fabrikant, Radiat. Eff. **46**, 85, 91 (1980).
[10] E. A. Kotomin and A. B. Doktorov, Phys. Status Solidi **114B**, 287 (1982).
[11] E. A. Kotomin, Proc. Latv. Acad. Sci. Phys. **N5**, 122 (1985).
[12] E. A. Kotomin and A. S. Chernov, Sov. Phys. Solid State **22**, 1575 (1980).
[13] E. A. Kotomin, DSc. thesis, Riga Institute of Physics of Latv. Acad. Sciences, 1988.
[14] P. V. Bochkanov, V. I. Korepanov, and V. M. Lisitsin, Proc. Sov. Higher Schools, Phys. **N3**, 16 (1989).
[15] N. Itoh, Adv. Phys. **31**, 491 (1972).
[16] M. Saidoh and N. Itoh, J. Phys. Chem. Solids **34**, 1165 (1973).
[17] N. Itoh and M. Saidoh, Phys. Status Solidi **33**, 649 (1969).
[18] K. K. Shwarts and Yu. A. Ekmanis, *Dielectric Materials: Radiation Processes and Radiation Stability* (Zinatne, Riga, 1989).
[19] V. N. Kuzovkov and E. A. Kotomin, Chem. Phys. **98**, 357 (1985).
[20] H. Eyring, S. H. Lin, and S. M. Lin, *Basic Chemical Kinetics* (Wiley, New York, 1980).
[21] A. I. Onipko, in *Physics of Many-Particle Systems* (Naukova Dumka, Kiev, 1982), Chap. 2, p. 60.

[22] T. R. Waite, Phys. Rev. **107**, 463 (1957).
[23] V. N. Kuzovkov, Sov. Theor. Expt. Chem. **21**, 33 (1985).
[24] V. N. Kuzovkov and E. A. Kotomin, Rep. Prog. Phys. **51**, 1479 (1988).
[25] V. L. Vinetski, Yu. H. Kalnin, E. A. Kotomin, and A. A. Ovchinnikov, Sov. Phys. Usp. **30**, N10, 1 (1990).
[26] Ya. B. Zeldovich, Sov. J. Electrochem. **13**, 677 (1977); A. A. Ovchinnikov and Ya. B. Zeldovich, Chem. Phys. **28**, 215 (1978).
[27] A. A. Ovchinnikov, S. F. Timashev, and A. A. Belyi, *Kinetics of Diffusion-Controlled Chemical Processes* (Nova Science, New York, 1989).
[28] *Proceedings of the International Conference on Non-Classical Kinetics* [J. Status Phys. **65**, 5/6 (1991)].
[29] A. Seeger, Radiat. Eff. Def. Solids **111/112**, 355 (1989).
[30] M. Zaiser, W. Frank, and A. Seeger, Solid State Phenom. **23/24**, 203 (1992).
[31] F. Leyvraz and S. Redner, Phys. Rev. Lett. **66**, 2168 (1991).
[32] I. M. Sokolov, H. Schnörer, and A. Blumen, Phys. Rev. A **44**, 2388 (1991).
[33] K. Linderberg, B. J. West, and R. Kopelman, Phys. Rev. Lett. **60**, 1777 (1988).
[34] S. Kanno, Prog. Theor. Phys. **79**, 721 (1988).
[35] V. Kuzovkov and E. Kotomin, Phys. Scr. **47** (1993).
[36] H. Taitelbaum, R. Kopelman, G. H. Weiss, and S. Havlin, Phys. Rev. A **41**, 3116 (1990).
[37] R. Schoonover, D. ben-Avraham, S. Havlin, R. Kopelman, and G. H. Weiss, Physica A **171**, 232 (1991).
[38] D. Toussaint and F. Wilczek, J. Chem. Phys. **78**, 2642 (1983).
[39] H. Schnörer, V. N. Kuzovkov, and A. Blumen, Phys. Rev. Lett. **63**, 805 (1989).
[40] H. Haken, *Synergetics* (Springer, Berlin, 1978).
[41] J. G. Kirkwood, J. Chem. Phys. **3**, 300 (1935).